DOI: 10.1002/ejic.200800540

The Use of Halide-Substituted Anilines for the Formation of Magnesium Imides

Jeffrey A. Rood,[a] Sondra E. Hinman,[a] Bruce C. Noll,[a] and Kenneth W. Henderson*[a]

Keywords: Magnesium / Imides / Amides / X-ray crystallography / Aggregation

The equimolar reactions of the halide-substituted anilines 2,4,6-trichloroaniline ($Ar_{Cl}NH_2$) and 2,3,4,5,6-pentafluoroaniline (Ar_FNH_2) with Bu_2Mg in the appropriate solvent system results in the formation of the magnesium imide compounds $[(Ar_{Cl}NMg{\cdot}thf)_4{\cdot}tol]$ (**4**), $[(Ar_{Cl}NMg{\cdot}diox)_4{\cdot}3diox]$ (**5**), $[(Ar_FNMg{\cdot}thf)_6{\cdot}3C_6H_6]$ (**6**) and $[(Ar_FNMg{\cdot}diox)_6]$ (**7**). Single-crystal X-ray diffraction analyses show that **4** and **5** adopt tetrameric cubane arrangements in the solid state, whereas **6** and **7** form prismatic hexameric aggregates. In comparison, reaction of 2 mol-equiv. of Ar_FNH_2 with Bu_2Mg produces the trimeric primary amide species $[\{(Ar_FNH)_6Mg_3{\cdot}(thf)_6\}{\cdot}2tol{\cdot}thf]$ (**9**). In addition, the serendipitous synthesis of the decametallic imide $[(Ar_FN)_9(F)_2Mg_{10}(thf)_6{\cdot}1.25tol]$ (**8a**) and the structural isomer $[(Ar_FN)_9(F)_2Mg_{10}(thf)_6{\cdot}4.5tol]$ (**8b**) were discovered during the attempted synthesis of **6**. It is presumed that the formation of these unusually large cage compounds results from the partial decomposition of the imide ligand by C–F bond cleavage. The compounds **8a** and **8b** have similar core-cage structures, but the orientation of their aryl groups and coordinated solvent molecules vary. The 20-vertex $Mg_{10}N_9F$ aggregates utilize one fluoride ion as a vertex, with a second fluoride ion encapsulated within the cage.
(© Wiley-VCH Verlag GmbH & Co. KGaA, 69451 Weinheim, Germany, 2008)

Introduction

Metal imides, "RNM", are known for a large number of metal systems, and have been found to form a variety of aggregated structures in the solid state.[1] Iminoalanes $(RNAlR')_n$ are one of the more widely studied groups of such compounds, where n = 2, 4, 6, 7, 8 etc.[2] In comparison, the imide chemistry of aluminum's periodic neighbor magnesium has been poorly investigated,[3] with only a handful of compounds having been structurally characterized. Power reported the synthesis and crystal structure of $[(PhNMg{\cdot}thf)_6]$ (**1**) in 1994.[4] Compound **1** was obtained from the reaction of Bu_2Mg with aniline in thf solution. The same group went on to characterize the compounds $[\{(1\text{-naphthyl})NMg{\cdot}thf\}_6{\cdot}2.25thf]$ (**2**) and $[\{(1\text{-naphthyl})NMg{\cdot}HMPA\}_6{\cdot}2tol]$ (**3**), derived from 1-naphthylamine.[5,6] All three complexes adopt similar prismatic hexameric arrangements in the solid state. Initial attempts to extend this class of compounds were hampered by the formation of unreactive bis(amide), $[RN(H)]_2Mg$, or alkyl(amide), RN(H)-MgR′, complexes.[7] It is believed that the weaker acidity of primary alkylamines and the steric encumbrance of 2,6-disubstituted anilines leads to the inability to remove the second proton from the amide. A recent report by Himmel et al. have shown that magnesium imide chemistry can be extended to amine ligands containing an α-silicon-stabilizing group. Specifically, the tetrameric cubane $[(Ph_3SiNMg{\cdot}thf)_4]$ was prepared by the reaction of the primary amine Ph_3SiNH_2 with Bu_2Mg.[8]

Our interest in magnesium imides lies in their potential use as preassembled secondary building units to construct metal-organic frameworks or coordination polymers.[9] We have demonstrated that divergent donor solvents may be used to link specific alkali-metal aggregates to create extended networks.[10] Magnesium imides are desirable candidates for this purpose, because solution dynamics of these polar complexes should be minimized due to the presence of strong Mg–N interactions.[11] In a recent communication, we reported the formation of the tetrameric magnesium imides $[(Ar_{Cl}NMg{\cdot}thf)_4{\cdot}tol]$ (**4**) and $[(Ar_{Cl}NMg{\cdot}diox)_4{\cdot}3(diox)]$ (**5**), where Ar_{Cl} = 2,4,6-$Cl_3C_6H_2$.[12] These halide-substituted compounds were formed at ambient temperature from the reaction of Bu_2Mg with the primary aniline. The ability to prepare these substituted anilides under mild conditions is presumably due to the relatively strong acidity of the amine substrate.[13] In this paper, we extend this work to the new ligand system 2,3,4,5,6-pentafluoroaniline, Ar_FNH_2. We present detailed solid-state structural results for the hexameric magnesium imides $[(Ar_FNMg{\cdot}thf)_6{\cdot}3C_6H_6]$ (**6**) and $[(Ar_FNMg{\cdot}diox)_6]$ (**7**) and include full data on the compounds **4** and **5** for comparative purposes. In addition, during these studies the unusually large magnesium imide clusters $[(Ar_FN)_9(F)_2Mg_{10}{\cdot}(thf)_6{\cdot}x(tol)]$ [x =

[a] Department of Chemistry and Biochemistry, University of Notre Dame,
Notre Dame, Indiana 46530, USA
Fax: +1-574-631-6652
E-mail: khenders@nd.edu

 © 2008 Wiley-VCH Verlag GmbH & Co. KGaA, Weinheim

1.25 (**8a**), 4.5 (**8b**)] were inadvertently prepared and are also described. Finally, we present the synthesis and crystal structure of the related magnesium bis(amide) complex [{$(Ar_FNH)_6Mg_3$·$(thf)_6$}·2tol·thf] (**9**).

Results and Discussion

Tetrameric Magnesium Imides

The previously reported complexes **4** and **5** are readily prepared by the equimolar reaction of the primary amine $Ar_{Cl}NH_2$ with Bu_2Mg (Scheme 1).[12] Recrystallization from the appropriate solvent mixtures allowed the preparation of high-quality single crystals, which were subsequently analyzed by X-ray diffraction. The crystal structures of **4** and **5** are presented in Figure 1. Both complexes adopt Mg_4N_4 cubane aggregates with each metal atom terminally solvated by a donor solvent (thf or 1,4-dioxane). The

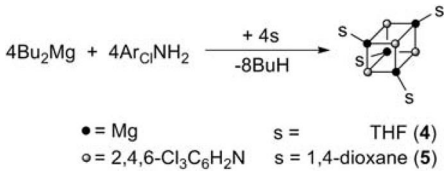

Scheme 1.

(a)

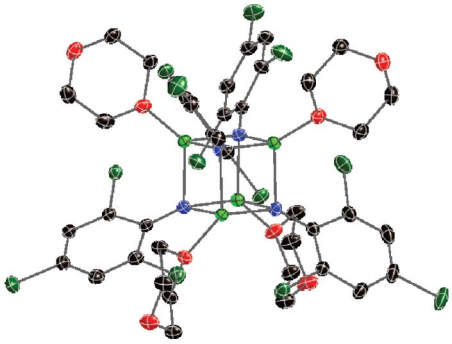

(b)

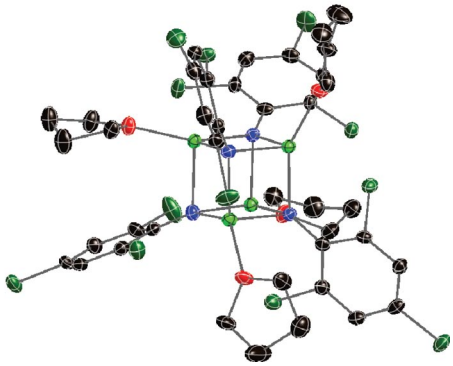

Figure 1. Molecular structures of tetrameric imides (a) **4** and (b) **5**, with lattice solvent molecules and H atoms omitted for clarity. Color code: Mg, light green; C, black; N, blue; O, red; Cl, dark green.

Table 1. Key bond lengths [Å] and angles [°] for **4**–**7**.

	4	**5**	**6**	**7**
Mg–N	2.110(2)	2.031(3)	2.0813(10)	2.024(4)
	2.080(2)	2.097(3)	2.0965(11)	2.064(4)
	2.066(2)	2.119(2)	2.0965(11)	2.118(3)
	2.128(2)	2.042(3)	2.0383(10)	2.047(4)
	2.079(2)	2.074(3)	2.0696(10)	2.054(4)
	2.063(2)	2.133(2)	2.1419(10)	2.109(3)
	2.158(2)	2.054(2)	2.0581(10)	2.079(4)
	2.117(2)	2.092(3)	2.0597(10)	2.080(4)
	2.048(2)	2.106(3)	2.0954(10)	2.099(3)
	2.122(2)	2.070(2)		
	2.079(2)	2.091(3)		
	2.072(2)	2.111(3)		
Mg–O	2.066(2)	2.059(2)	2.0412(9)	2.064(3)
	2.055(2)	2.061(2)	2.0307(10)	2.042(3)
	2.038 (2)	2.052(2)	2.0299(10)	2.070(3)
	2.070(2)	2.052(2)		
C_{aryl}–N	1.339(3)	1.328(3)	1.3648(14)	1.362(5)
	1.337(3)	1.336(4)	1.3597(14)	1.365(5)
	1.330(3)	1.332(4)	1.3582(14)	1.375(8)
	1.334(3)	1.333(3)		
N–Mg–N	92.04(9)	92.04(10)	112.07(4)	124.06(15)
	91.64(9)	91.48(10)	93.43(4)	94.04(14)
	89.43(9)	91.05(9)	93.79(4)	91.19(14)
	92.42(9)	92.44(10)	124.53(4)	119.88(15)
	92.27(9)	90.78(9)	94.23(4)	91.88(14)
	88.64(9)	90.27(10)	90.94(4)	94.52(14)
	91.23(9)	92.49(10)	121.66(4)	113.17(14)
	91.70(9)	91.58(10)	94.24(4)	94.09(14)
	91.25(9)	90.07(10)	92.55(4)	92.98(14)
	90.93(9)	92.06(10)		
	93.15(9)	91.99(9)		
	89.88(9)	89.99(10)		
Mg–N–Mg	90.02(9)	90.56(10)	113.82(5)	120.59(17)
	88.52(9)	87.95(9)	87.26(4)	88.36(13)
	88.99(9)	88.61(10)	86.40(4)	85.24(13)
	90.56(9)	89.59(10)	121.84(5)	115.66(16)
	86.41(9)	88.80(10)	88.75(4)	87.43(14)
	88.92(9)	87.56(9)	85.92(4)	86.13(13)
	89.71(9)	88.92(10)	124.11(5)	124.68(17)
	88.14(9)	88.91(9)	87.75(4)	88.56(13)
	88.76(8)	87.61(9)	84.71(4)	85.52(13)
	88.14(9)	87.50(9)		
	86.59(8)	89.30(9)		
	90.24(9)	88.22(10)		

Mg_4N_4 cubane motif is notable, with the only known related compounds being the phosphoraniminato complex $[(Me_3PNMgBr)_4]$[14] and the recently reported magnesium imide $[(Ph_3SiNMg·thf)_4]$.[8,15] Computational studies (HF/6-31G*) support that a combination of steric factors, including metal solvation, lead to the thermodynamic preference for the tetrameric cubane arrangements adopted for **4** and **5**.[12] The calculations also indicated that formation of an extended network through bridging dioxane in **5** is energetically unfavorable due to steric interactions between neighboring aggregates.

A detailed list of key bond lengths and angles for **4** and **5** are shown in Table 1. The average Mg–N distance is 2.094(2) Å for **4**, and 2.085(2) Å for **5**. The average Mg–O distances are 2.057(2) Å and 2.061(2) Å for **4** and **5**, respectively. The aggregates deviate only slightly from ideal cubes, with internal N–Mg–N bond angles ranging from 88.64(9)

 © 2008 Wiley-VCH Verlag GmbH & Co. KGaA, Weinheim

to 93.15(9)° in **4** and from 90.00(8) to 92.46(8)° in **5**. Similarly, the internal Mg–N–Mg angles cover the narrow range between 86.41(9) and 90.56(9)° in **4** and between 87.50(9) and 90.56(10) in **5**. The silyl-substituted complex $[(Ph_3SiNMg{\cdot}thf)_4]$ has a mean Mg–N distance of 2.090(3) Å, similar to those of **4** and **5**. However, the mean Mg–O distance is slightly shorter at 2.010(3) Å, suggesting less local steric encumbrance near the metal atoms in the silyl complex. The cubane is also slightly more distorted than in **4** and **5**, with N–Mg–N and Mg–N–Mg angles ranging between 84.29(12) and 84.82(12) and between 94.88(12) and 95.52(12)°.

Hexameric Magnesium Imides

Following these studies, we were attracted to the possibility of readily forming other halide-substituted magnesium imides. We opted to investigate the use of 2,3,4,5,6-pentafluoroaniline as a substrate, because it should be relatively acidic, and also the small fluoro substituents may allow the formation of an extended net. First, the equimolar reaction of Bu_2Mg with Ar_FNH_2 was carried out in benzene at ambient temperature and resulted in the formation of a white precipitate (Scheme 2). The solid was solublized on addition of thf followed by heating of the mixture to reflux. (***Caution:*** Great care should be taken when preparing and handling reactive fluorinated organometallics due to the possibility of explosive C–F cleavage![16]) Slow cooling afforded high-quality crystals. ^1H and ^{13}C NMR spectroscopic analyses in $[D_8]$thf indicated the presence of only thf and residual benzene, indicative of complete imide formation, i.e. the absence of alkyl or N(H) signals was suggestive of double alkane elimination.

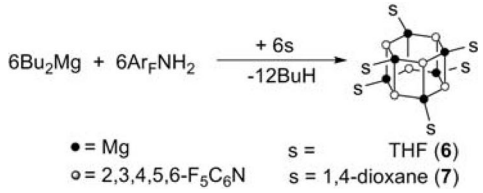

Scheme 2.

A single-crystal X-ray diffraction experiment confirmed the successful synthesis of the magnesium imide $[(Ar_FNMg{\cdot}thf)_6{\cdot}3C_6H_6]$ (**6**). As shown in Figure 2 (a), the complex adopts a prismatic hexameric arrangement in the solid state. The six Mg centers are bridged through six μ_3-Ar_FN^{2-} ligands. Tetracoordination of each metal atom is completed through terminal solvation by thf.

Next, a similar reaction was conducted with the single change of replacing thf with 1,4-dioxane. Again, high-quality crystals were prepared, and their ^1H and ^{13}C NMR spectroscopic data were suggestive of imide formation similar to **6**. A single-crystal X-ray diffraction experiment revealed the prismatic hexameric aggregate $[(Ar_FNMg{\cdot}diox)_6]$ (**7**) [Figure 2 (b)].

Thus, the reduction in steric hindrance on changing from chloro- to fluoro-substituted anilines has the effect of stabilizing the larger hexameric aggregates in favor of the tetrameric aggregates found for **4** and **5**. Also, the formation of a molecular complex, rather than a dioxane-bridged network, is presumably due to repulsive interaggregate interactions.

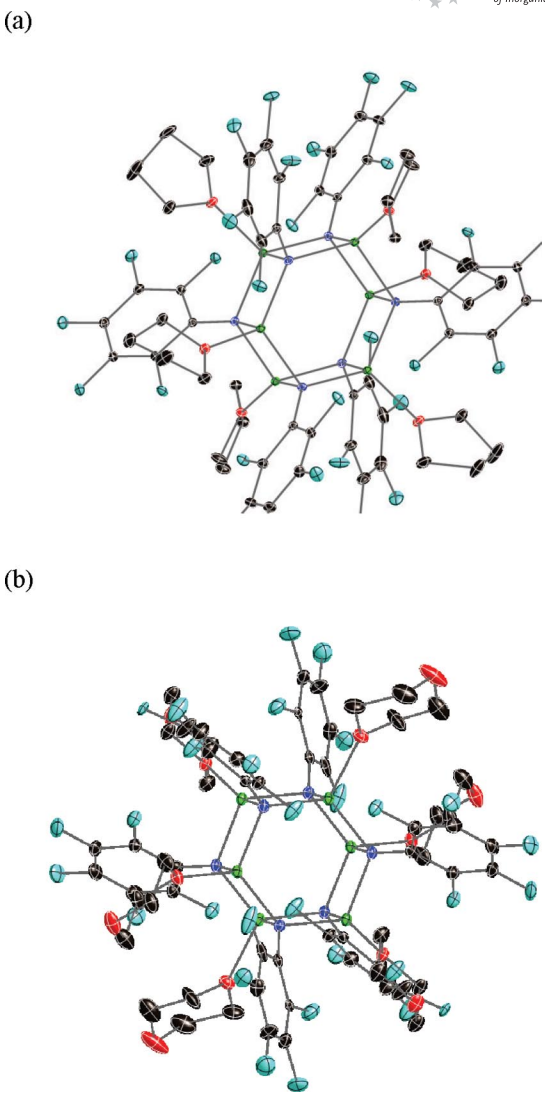

Figure 2. Molecular structures of hexameric imides: (a) **6**, (b) **7**, with lattice solvent molecules and H atoms omitted for clarity. Color code: Mg, light green; C, black; N, blue; O, red; F, teal.

The overall structural arrangements in **6** and **7** are very similar, and details are given in Table 1. The average Mg–N distances are 2.082(1) Å for **6** [range 2.038(1)–2.142(1) Å], and 2.075(4) Å for **7** [range 2.024(4)–2.118(4) Å]. These average values are close to those reported for the prismatic hexamers **1**–**3** at 2.061, 2.064, and 2.079 Å, respectively.[4,5] The average Mg–O distances for **6** and **7** of 2.033(1) and 2.059(3) Å are also similar to those of **1** and **2** at 2.028 and 2.019 Å, respectively. A much smaller average Mg–O distance of 1.963 is found in **3** as a consequence of the stronger binding to the highly Lewis basic donor HMPA. An interesting distance for comparison within the seven complexes **1**–**7** is the *ipso*-carbon–imido-

 © 2008 Wiley-VCH Verlag GmbH & Co. KGaA, Weinheim

nitrogen bond length. The N–C distance in aniline is 1.392 Å.[17] The mean C–N distances for the three simple anilides **1**, **2** and **3** are 1.386, 1.368 Å and 1.383 Å respectively. The chloro-substituted derivatives **4** and **5** have mean C–N distances of 1.335(3) and 1.332(3) Å, and the fluoro-substituted derivatives **6** and **7** have these distances at 1.3609(14) and 1.367(5) Å. The short distances found in **4** and **5** are consistent with substantial back-donation of the charge into the aromatic systems of these molecules. This shortening is less pronounced for the fluoro-substituted complexes **6** and **7**.

Considering the bond angles within **6** and **7**, both complexes form slightly distorted hexameric prisms. The mean N–Mg–N and Mg–N–Mg bond angles within the "hexagonal" Mg_3N_3 rings of the cages are 119.42(4) and 119.92(4)° for **6** and 119.01(14) and 120.31(13)° for **7**. Also, the mean N–Mg–N and Mg–N–Mg bond angles within the "square" Mg_2N_2 rings are 93.20(4) and 86.80(4)° for **6** and 93.12(14) and 86.88(13)° for **7**.

Solution NMR spectroscopic studies of **4**–**7** provided only limited information. The ^1H and ^{13}C NMR spectra of **4** and **5** in [D_5]pyridine displayed a single set of aromatic resonances, along with the coordinated and included solvent. For **6** and **7**, ^{19}F NMR spectra in [D_8]thf provide the only useful data, displaying a single set of somewhat broad fluoride resonances at δ = –162.93, –170.01 and –188.32 ppm, representative of the *ortho*-, *meta*-, and *para*-F atoms on an aromatic ring.[18] A variable-temperature ^{19}F NMR spectroscopic study was carried out on a sample of **6** in [D_8]thf between –60 and +60 °C with a 600 MHz spectrometer. A single set of signals was observed throughout this temperature range, and no discernible splitting of the peaks was noted. Also, the chemical shifts of the signals varied by < 0.6 ppm over this entire temperature range. These data are consistent with single, highly symmetrical aggregates in solution, similar to those seen in the solid state. Alternatively, it is possible that there is fast exchange between multiple aggregates in solution, but this seems unlikely given the expected strength of the bonding within the cage cores.[8]

Decametallic Magnesium Imides

The unexpected product [$(Ar_FN)_9(F)_2Mg_{10}$·$(thf)_6$·1.25tol] (**8a**) was characterized by a single-crystal X-ray diffraction experiment during an attempted repeat synthesis of hexameric imide **6**. Several batches of crystals were prepared under various conditions in an attempt to reproduce the synthesis of **8a** as a bulk material for further analyses. This did result in the synthesis of the structural isomer [$(Ar_FN)_9$-$(F)_2Mg_{10}$·$(thf)_6$·4.5tol] (**8b**), which was also successfully characterized by crystallography. However, the bulk material produced was consistently compound **6**, as determined by ^{19}F NMR analyses. The single crystals of **8a** and **8b** are therefore minor side products, and their analytical data are limited to their crystallographic characterization. Nevertheless, **8a** and **8b** are interesting compounds worthy of comment.

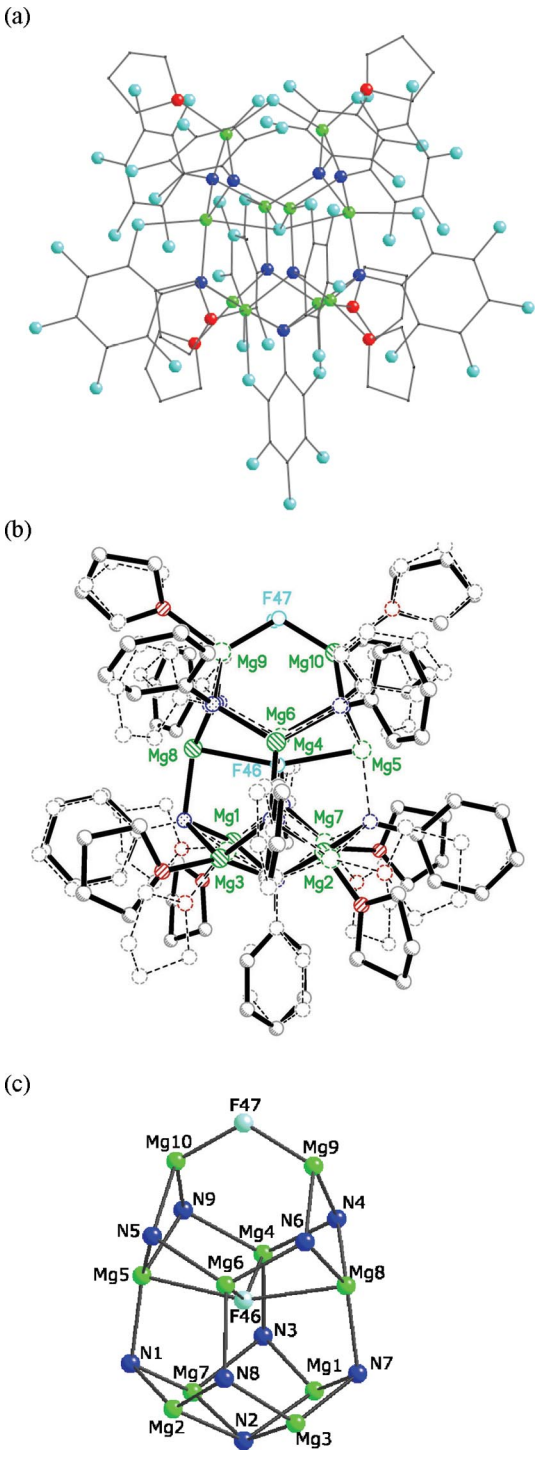

Figure 3. (a) Molecular structure of **8a** with lattice solvent molecules and H atoms omitted for clarity. (b) Superimposed images of **8a** (solid) and **8b** (dotted) showing the similarity in the cage cores and the differences in the relative orientations of the aryl rings and coordinated thf molecules. Aryl–F and H atoms are omitted for clarity. (c) $Mg_{10}N_9F_2$ cage structure **8a**, with the encapsulated F46 atom at its core. Color code: Mg, light green; C, black; N, blue; O, red; F, teal.

Figure 3 shows the molecular structure of **8a**. The structure consists of ten metal centers, nine aromatic imide groups and two fluoride ions. It is important to note that

 © 2008 Wiley-VCH Verlag GmbH & Co. KGaA, Weinheim

the refinements of both **8a** and **8b** indicated small amounts of residual electron density close to the cluster-capping F47 atom (approximately one two-electron site and two single-electron sites). This is likely due to partial occupancy of this site by another anion, such as an alkoxide stemming from the Bu_2Mg source or from decomposition of the thf solvent. We have previously reported an ether cleavage product in reactions involving Bu_2Mg with substituted anilines.[7b] The refinement of both **8a** and **8b** therefore contains our best guess as partially occupied enolate of acetaldehyde. For simplicity, this disorder has been removed in the figures.

The cage cores of the two compounds are almost identical, but they differ in the orientations of the aryl rings and attached thf molecules [Figure 3 (b)]. The overall quality of the refinement of compound **8b** is rather poor (R_1 = 11.5%), and thus the following discussion is limited to that of **8a**.

The structure and composition of **8a** is intriguing. The cage structure is novel and can be described as a 20-vertex $Mg_{10}N_9F$ polygon composed of four Mg_3N_3 six-membered rings, two Mg_3N_2F six-membered rings, and six four-membered Mg_2N_2 rings [Figure 3 (c)]. Discrete cage compounds containing more than six magnesium centers are very rare,[6a,19] and to the best of our knowledge **8a** is the first example of a compound containing ten magnesium atoms to be structurally characterized.[20] Four of the metal atoms (Mg1, Mg2, Mg3 and Mg7) bind to two μ_3-N atoms, one μ_4-N atom, and the oxygen atom of a thf molecule. The two metal atoms Mg9 and Mg10 each bind to two μ_3-N atoms, the oxygen atom of a thf molecule, and also to the vertex F47 atom. The remaining four metal atoms (Mg4, Mg5, Mg6 and Mg8) are located in the central section of the cage. Two of the metal atoms (Mg4 and Mg6) bind to three μ_3-N atoms and the encapsulated F46 atom. The two other metal atoms (Mg5 and Mg8) similarly bind to three μ_3-N atoms but make substantially longer contacts to the encapsulated F46 atom (details of the metrical parameters are given below).

The presence of fluoride anions is unexpected and is likely a consequence of partial decomposition of the anilide through C–F bond cleavage reactions. Significant precedent exists for related aryl C–F bond-cleavage reactions.[21] However, only a relatively small number of molecular alkali or alkaline earth metal complexes containing direct metal–fluoride interactions have been characterized in the solid state.[20] Indeed, only a handful of compounds containing Mg–F interactions have been reported in the Cambridge Structural Database.[22] On reflection, this is not surprising, due to the high lattice enthalpy for MgF_2 salt formation. In this case incorporation of the fluoride anions within the sterically well-protected cage aggregate may help to prevent salt formation.

Next, the analysis of the bond lengths and angles within **8a** show close similarities with the other characterized magnesium imides. In **8a** the mean Mg–N bond length is 2.081(11) Å, the N–Mg–N angles range between 90.5(4) and 132.2(5)°, and the Mg–N–Mg angles range between 80.2(4) and 140.9(5)°. The angles are consistent with those found for the related four- or six-membered rings in complexes **1**–**7**.

The Mg–F bond lengths around the cluster-capping, μ_2-vertex F47 atom should be viewed with caution due to the disorder at this site. In any event, the Mg–F distances in **8a** are estimated to be 1.759(28) Å to Mg9, and 1.902(27) Å to Mg10. The encapsulated F46 atom has two close contacts of 2.006(10) Å to Mg4 and 2.005(10) to Mg6. The next closest contacts to F46 are to the two metal atoms Mg5 and Mg8, with distances of 2.385(10) and 2.449(10) Å. For comparison, the only other homometallic magnesium compound that has been structurally characterized containing Mg–F bonds is the β-diketiminate [{{CH(CMeNAr′)$_2$}-Mg(μ_2-F)·(thf)}$_2$·tol] (Ar′ = 2,6-*i*Pr$_2$C$_6$H$_3$).[22d] The structure is composed of a central Mg_2F_2 ring, with an Mg–F distance of 1.9507(17) Å.

A final point of note in the structure of **8a** is the presence of a number of close aryl fluoride–metal contacts. Eight of the ten metal atoms have an Mg–F_{Ar} contact of < 2.3 Å. These interactions are likely weak at best, but it is interesting to note their presence as potential precursors to C–F bond cleavage.

Trimeric Magnesium Primary Bis(amide)

Attempts to prepare **8a** or **8b** as pure compounds included variation of the reaction time, reaction temperature, the solvent media utilized and also the ratio of Bu_2Mg/primary amine. The use of two mol-equiv. of amine to the metal base resulted in the preparation of the primary bis(amide) species [{(Ar$_F$NH)$_6$Mg$_3$·(thf)$_6$}·2tol·thf] (**9**). Compound **9** was characterized in the solid state and found to adopt an unusual trimeric aggregate as shown in Figure 4. Two different magnesium environments are present in **9**. The central metal is octahedrally coordinated to six amide ligands, whereas the two outer metal atoms bind to three amide groups and three thf molecules. The closest structural analogue to **9** is the calcium arylamide [(MesNH)$_6$-Ca$_3$·(thf)$_6$], (Mes = 2′,4′,6′-Me$_3$C$_6$H$_2$) recently reported by Westerhausen.[23] Molecular trimers of magnesium are somewhat scarce,[24] and the structural motif of each metal

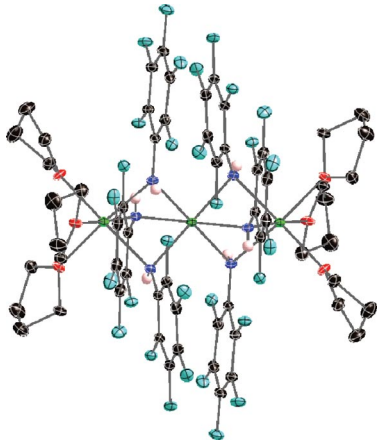

Figure 4. Molecular structure of **9** with lattice solvent molecules and non-amido H atoms omitted for clarity. Color code: Mg, light green; C, black; N, blue; O, red; F, teal; H, pink.

 © 2008 Wiley-VCH Verlag GmbH & Co. KGaA, Weinheim

atom bridged by three μ_2-anions is particularly rare. This arrangement requires the anions to be relatively compact, as is also seen in the complex $[(PhS)_6Mg_3{\cdot}(pyr)_6]$.[25]

The metrical data within **9** are in accord with expectations for a magnesium bis(amide) (Table 2).[26] The mean Mg–N bond length is 2.206(2) Å, with a range of 2.176(2)–2.237(2) Å. These bonds are ca. 0.1 Å longer than those in **6** and **7** as a consequence of the single anionic charge present on the nitrogen atoms in **9**. The mean N–Mg–N bond angle is 81.25(6)° [range 79.90(6)–82.61(6)°], and the Mg–N–Mg bond angles are all 82.48(7)° due to symmetry. The amido proton was located in the difference Fourier map from the X-ray diffraction experiment.

Table 2. Key bond lengths [Å] and angles [°] for **9**.

Mg–N	2.2369(16)
	2.1761(18)
Mg–O	2.168(2)
N–Mg–N	180.00
	100.10(6)
	79.90(6)
	82.61(7)
Mg–N–Mg	82.48(6)

The ^{1}H NMR spectrum of **9** in $[D_8]$thf solution confirms the presence of the primary amide proton by a signal at δ = 2.87 ppm, along with signals for thf and the toluene of crystallization. The ^{19}F NMR spectrum of this compound displays a single set of signals at δ = –169.85, –170.11 and –191.95 ppm arising from the *ortho*-, *meta*-, and *para*-F atoms on the aromatic rings. These values are shifted slightly upfield compared to those of imides **6** and **7**.

Conclusions

Our studies illustrate that halide-substituted primary anilines may be used as substrates for the formation of magnesium imide complexes. The resulting aggregation state of the magnesium imide product depends on the local steric environment of the ligand at the 2- and 6-positions of the aromatic ring. Solvation also plays an important role in stabilizing the aggregate adopted.[12]

Use of the fluoro-substituted aryl ligands in these reactions is accompanied by the possibility of C–F bond cleavage. This is likely the reason for the formation of the novel decametallic aggregates **8a** and **8b**. The ability to form such unusually large aggregates for a magnesium complex is due to the presence of the small fluoride vertex, and also as the imide ligands carry a formal double negative charge, allowing a single anionic partner per metal atom.

Magnesium imide cages remain attractive candidates as discrete secondary building units for the formation of metal-organic frameworks. In the present study 1,4-dioxane appears to be too short of a linker to overcome interaggregate repulsions between the specific magnesium imide cages, resulting the in formation of molecular complexes. Current studies are underway to investigate the use of other acidic primary amine ligands, as well as other divergent linker molecules, for the formation of extended nets.

Experimental Section

General: All experimental manipulations were performed under an inert gas by using standard Schlenk techniques. 1,4-Dioxane was distilled from sodium benzophenone ketyl and stored over molecular sieves (4 Å) prior to use. Benzene was dried with CaH_2 and distilled onto molecular sieves (4 Å) prior to use. Toluene and thf were purified by passage through a solvent purification system (Innovative Technology). Bu_2Mg was supplied as a 1.0 M solution in heptane from Aldrich and standardized prior to use. 2,3,4,5,6-Pentafluoroaniline was recrystallized from *n*-hexane. The NMR spectra were recorded with a Varian-300 spectrometer at 293 K. The variable-temperature ^{19}F NMR spectroscopic study on **6** was carried out between –60 and +60 °C with a Varian DirectDrive-600 spectrometer. ^{1}H and ^{13}C NMR spectra were referenced internally to the residual signals of the deuterated solvent, and ^{19}F NMR spectra were externally referenced to $CFCl_3$. FTIR spectra were obtained from Nujol mulls with a Perkin–Elmer Paragon 1000 FTIR spectrometer in the range of 4000–650 cm^{-1}. ***Caution:*** It has been noted in the literature that organometallic compounds containing electropositive metals and aromatic fluorides are potential explosive hazards and should be handled with great care![16] On one occasion during the present study, exposure of a residual portion of **6** to air resulted in explosion. Melting points and elemental analyses of these compounds were therefore not determined.

$[(Ar_FNMg{\cdot}thf)_6{\cdot}3C_6H_6]$ (6): 2,3,4,5,6-Pentafluoroaniline (0.183 g, 1 mmol) was dissolved in benzene (4 mL). Bu_2Mg (1 mmol of a 1.0 M solution in heptane) was added dropwise to the mixture, and a white precipitate formed. The mixture was heated to reflux temperature, and the precipitate was solublized upon addition of thf (1 mL). The hot solution was cooled slowly in a hot water bath overnight, affording a batch of clear, colorless crystals of **6**. Yield: 0.217 g, 68%. ^{1}H NMR (300 MHz, $[D_8]$thf): δ = 7.30 (s, Ar-H, benzene), 3.62 (m, OCH_2, thf), 1.74 (m, CH_2, thf) ppm. ^{19}F NMR (282 MHz, $[D_8]$thf): δ = –162.93 (m, *ortho*-F), –170.01 (m, *meta*-F), –188.32 (m, *para*-F) ppm. FTIR (Nujol): $\tilde{\nu}$ = 2366 (w), 1633 (w), 1601 (w), 1510 (m), 1493 (s), 1462 (m), 1425 (s), 1285 (w), 1233 (m), 1150 (m), 1000 (s), 969 (s), 881 (w), 730 (w) cm^{-1}.

$[(Ar_FNMg{\cdot}diox)_6]$ (7): 2,3,4,5,6-Pentafluoroaniline (0.183 g, 1 mmol) was dissolved in benzene (4 mL). Bu_2Mg (1 mmol of a 1.0 M solution in heptane) was added dropwise to the mixture, and a white precipitate formed. The reaction mixture was heated to reflux, and the precipitate was solublized upon addition of 1,4-dioxane (3 mL). The hot solution was cooled slowly in a hot water bath, affording a batch of clear, colorless crystals of **7**. Yield: 0.231 g, 78%. ^{1}H NMR (300 MHz, $[D_8]$thf): δ = 3.64 (s, OCH_2, 1,4-dioxane) ppm. ^{19}F NMR (282 MHz, $[D_8]$thf): δ = –162.93 (m, *ortho*-F), –170.01 (m, *meta*-F), –188.32 (m, *para*-F) ppm. FTIR (Nujol): $\tilde{\nu}$ = 2364 (w), 1633 (w), 1603 (w), 1510 (m), 1491 (s), 1425 (s), 1285 (w), 1233 (m), 1150 (m), 1084 (w), 1049 (m), 1000 (s), 969 (s), 881 (w), 730 (w) cm^{-1}.

$[(Ar_FN)_9(F)_2Mg_{10}{\cdot}(thf)_6{\cdot}x(tol)]$ [x = 1.25 (8a), 4.5 (8b)]: 2,3,4,5,6-Pentafluoroaniline (0.183 g, 1 mmol) was dissolved in toluene (4 mL). Bu_2Mg (1 mmol of a 1.0 M solution in heptane) was added dropwise to the mixture, and a white precipitate formed. The solution was heated at reflux for 45 min, upon which the color changed to an orange-brown. The solid was solublized with thf and cooled slowly to give crystals of either **8a** or **8b**. Analyses were limited to single-crystal X-ray diffraction.

$[\{(Ar_FNH)_6Mg_3{\cdot}(thf)_6\}{\cdot}2tol{\cdot}thf]$ (9): 2,3,4,5,6-Pentafluoroaniline (0.366 g, 2 mmol) was dissolved in toluene (4 mL). Bu_2Mg (1 mmol of a 1.0 M solution in heptane) was added dropwise to the mixture,

 © 2008 Wiley-VCH Verlag GmbH & Co. KGaA, Weinheim

and a white precipitate formed. The solution was heated to reflux temperature for 45 min, upon which the color changed to an orange-brown. The solid was solublized with thf (1 mL). Slow cooling of the mixture led to high-quality crystals of **9**. Yield 0.323 g, 52%. ^{1}H NMR (300 MHz, [D$_8$]thf): δ = 7.2–7.4 (m, Ar-H, toluene), 3.62 (m, OCH$_2$, thf), 2.87 (s, NH), 2.30 (s, CH$_3$, toluene), 1.72 (m, CH$_2$, thf) ppm. ^{19}F NMR (282 MHz, [D$_8$]thf): δ = –169.85 (m, *ortho*-F), –170.11 (m, *meta*-F), –191.95 (m, *para*-F) ppm. FTIR (Nujol): $\tilde{\nu}$ = 3393 (w), 2355 (w), 1669 (w), 1648 (w), 1607 (w), 1510 (s), 1456 (s), 1373 (m), 1238 (w), 1166 (w), 1119 (w), 994 (m), 942 (m), 834 (w), 720 (m) cm^{-1}.

X-ray Crystallography: Single crystals were examined under Infineum V8512 oil. The datum crystal was affixed to either a thin glass fiber atop a tapered copper-mounting pin or Mitegen mounting loop and transferred to the 100 K nitrogen stream of a Bruker APEX II diffractometer equipped with an Oxford Cryosystems 700 series low-temperature apparatus. Cell parameters were determined

Table 3. Crystallographic data for **4**–**9**.

	4	**5**	**6**	**7**
Empirical formula	$C_{52}H_{64}Cl_{12}Mg_4N_4O_{14}$	$C_{47}H_{48}Cl_{12}Mg_4N_4O_4$	$C_{84}H_{72}F_{30}Mg_6N_6O_6$	$C_{60}H_{40}F_{30}Mg_6N_6O_{12}$
Formula mass	1491.71	1255.53	1977.34	1752.84
T [K]	100(2)	100(2)	100(2)	100(2)
Crystal system	triclinic	monoclinic	triclinic	monoclinic
Space group	$P\bar{1}$	$P2_1/n$	$P\bar{1}$	$P2_1/n$
a [Å]	13.922(3)	16.3452(2) Å	12.6733(8)	11.3659(5)
b [Å]	15.111(3)	12.8441(2)	14.2803(8)	22.8286(13)
c [Å]	17.506(4)	25.5481(4)	14.6238(12)	13.0987(8)
α [°]	67.57(3)	90	106.648(4)	90
β [°]	81.47(3)	94.438(1)	114.373(3)	99.871(2)
γ [°]	73.71(3)	90	100.841(3)	90
V [Å^3]	3264.0(11)	5347.47(13)	2162.7(3)	3348.4(3)
Z	2	4	2	2
D [Mg/m^3]	1.513	1.560	1.518	1.739
μ (Mo-K_α) [mm^{-1}]	0.611	0.654	0.178	0.224
Crystal size [mm]	0.39 × 0.23 × 0.21	0.27 × 0.25 × 0.24	0.46 × 0.39 × 0.38	0.37 × 0.17 × 0.16
T_{max}, T_{min}	0.83, 0.88	0.83, 0.87	0.93, 095	0.95, 0.98
θ_{min}, θ_{max} [deg]	1.26, 26.37	3.10, 66.49	1.59, 31.83	1.78, 25.19
Reflections	88818	38948	83570	44631
Independent reflections	13330	8869	14570	5933
R(int)	0.0301	0.0372	0. 0297	0.0380
R_1,[a] wR_2[b] [$I>2\sigma(I)$]	0.0482, 0.1418	0.0357, 0.0862	0.0421, 0.1074	0.0666, 0.1852
R_1,[a] wR_2[b] (all data)	0.0515, 0.1473	0.0474, 0.0921	0.0558, 0.1210	0.0948, 0.2108
GOOF (F^2)	1.025	1.017	1.049	1.075
Largest peak, hole [e Å^{-3}]	1.141, –1.225	1.171, –0.365	0. 794, –0.595	0.781, –0.523
	8a	**8b**	**9**	
Empirical formula	$C_{88.19}H_{60.88}F_{46.28}Mg_{10}N_9O_{6.28}$	$C_{110.52}H_{86.04}F_{46.49}Mg_{10}N_9O_{6.51}$	$C_{78}H_{78}F_{30}Mg_3N_6O_7$	
Formula mass	2472	2765.75	1852.62	
T [K]	100(2)	100(2)	100(2)	
Crystal system	triclinic	monoclinic	rhombohedral	
Space group	$P\bar{1}$	$P2_1/n$	$R\bar{3}c$	
a [Å]	13.5899(13)	13.6134(8)	19.8192(7)	
b [Å]	17.4743(8)	29.5004(19)	19.8192(7)	
c [Å]	22.5672(17)	25.8985(17)	34.4967(15)	
α [°]	79.557(2)	90	90.00	
β [°]	83.612(6)	90.030(4)	90.00	
γ [°]	81.566(6)	90	120.00	
V [Å^3]	5189.7(7)	10400.9(11)	11734.9(8)	
Z	2	4	6	
D [Mg/m^3]	1.557	1.630	1.505	
μ (Mo-K_α) [mm^{-1}]	0.205	0.217	0.169	
Crystal size [mm]	0.31 × 0.33 × 0.42	0.26 × 0.27 × 0.38	0.37 × 0.29 × 0.26	
T_{max}, T_{min}	0.93, 0.95	0.94, 0.96	0.95, 0.98	
θ_{min}, θ_{max} [deg]	2.22, 25.22	2.21, 25.98	1.67, 28.46	
Reflections	18334	112645	3302	
Independent reflections	18334	12524	2449	
R(int)	0.0847	0.0807	0.0390	
R_1,[a] wR_2[b] [$I>2\sigma$ (I)]	0.0770, 0.1868	0.1152, 0.3019	0.0545, 0.1451	
R_1,[a] wR_2[b] (all data)	0.1255, 0.2306	0.1614, 0.3243	0.0766, 0.1719	
GOOF, F^2[c]	1.152	1.052	1.052	
Largest peak, hole [e Å^{-3}]	1.156, –0.565	1.036, –0.804	0.845, –0.584	

[a] $R1 = \Sigma||F_o| - |F_c||/\Sigma|F_o|$. [b] $wR2 = \{\Sigma|w(F_o^2 - F_c^2)^2|/\Sigma|w(F_o^2)^2|\}^{1/2}$, $w^{-1} = [(\sigma^2F_o^2) + (0.1325P)^2 + 9.6648P]$, $P = (F_o^2 - 2F_c^2)/3$. [c] GOOF = $S = [\Sigma|w(F_o^2 - F_c^2)^2|/(n - p)]^{1/2}$, n = number of reflections, p = number of parameters.

 © 2008 Wiley-VCH Verlag GmbH & Co. KGaA, Weinheim

by using reflections harvested from three sets of 12 0.5° ϕ scans. The orientation matrix derived from this was transferred to COSMO[27] to determine the optimum data collection strategy requiring a minimum of fourfold redundancy. Cell parameters were refined by using reflections harvested from the data collection with $I \geq 10\sigma(I)$. All data were corrected for Lorentz and polarization effects, and runs were scaled by using SADABS.[28] The structures were solved from partial datasets by using the Autostructure option in APEX 2.[23] This option employs an iterative application of the direct methods, Patterson synthesis, and dual-space routines of SHELXTL.[29] Hydrogen atoms were placed at calculated geometries and allowed to ride on the position of the parent atom. Crystallographic details are available in Table 3. CCDC-689290 (**6**), -689291 (**8b**), -689292 (**8a**), -689293 (**9**), and -689294 (**7**) contain the supplementary data for this paper. These data can be obtained from the Cambridge Crystallographic Data Centre via www.ccdc.ac.uk/data_request/cif.

Acknowledgments

We gratefully acknowledge the Petroleum Research Fund (41716-AC3) and the National Science Foundation (Grant CHE-0443233) for support.

[1] a) M. Veith, *Angew. Chem. Int. Ed. Engl.* **1987**, *26*, 1–14; b) M. Veith, *Chem. Rev.* **1990**, *90*, 3–16.
[2] S. Schulz, F. Thomas, W. M. Priesmann, M. Nieger, *Organometallics* **2006**, *25*, 1392–1398, and references therein.
[3] E. C. Ashby, G. F. Willard, *J. Org. Chem.* **1978**, *43*, 4750–4758.
[4] T. Hascall, K. Ruhlandt-Senge, P. P. Power, *Angew. Chem. Int. Ed. Engl.* **1994**, *33*, 356–357.
[5] a) W. J. Grigsby, T. Hascall, J. J. Ellison, M. M. Olmstead, P. P. Power, *Inorg. Chem.* **1996**, *35*, 3254–3261; b) W. J. Grigsby, M. M. Olmstead, P. P. Power, *J. Organomet. Chem.* **1996**, *513*, 173–180.
[6] The mixed halide/imide complex $[\{(Et_2O)Mg\}_6(NPh)_4Br_4]$ has also been reported: a) T. Hascall, M. M. Olmstead, P. P. Power, *Angew. Chem. Int. Ed. Engl.* **1994**, *33*, 1000–1001.
[7] a) M. M. Olmstead, W. J. Grigsby, D. R. Chacon, T. Hascall, P. P. Power, *Inorg. Chim. Acta* **1996**, *251*, 273–284; b) J. A. Rood, B. C. Noll, K. W. Henderson, *Inorg. Chem. Commun.* **2006**, *9*, 1129–1132.
[8] A. Fuchs, E. Kaifer, H.-J. Himmel, *Eur. J. Inorg. Chem.* **2008**, 41–43.
[9] a) K. W. Henderson, A. R. Kennedy, A. E. McKeown, D. S. Strachan, *J. Chem. Soc., Dalton Trans.* **2000**, 4348–4353; b) K. W. Henderson, A. R. Kennedy, D. J. MacDougall, D. Shanks, *Organometallics* **2002**, *21*, 606–616; c) K. W. Henderson, A. R. Kennedy, L. MacDonald, D. J. MacDougall, *Inorg. Chem.* **2003**, *42*, 2839–2841.
[10] a) D. J. MacDougall, J. J. Morris, B. C. Noll, K. W. Henderson, *Chem. Commun.* **2005**, 456–458; b) D. J. MacDougall, B. C. Noll, K. W. Henderson, *Inorg. Chem.* **2005**, *44*, 1181–1183; c) J. J. Morris, B. C. Noll, K. W. Henderson, *Cryst. Growth Des.* **2006**, *6*, 1071–1073; d) J. J. Morris, B. C. Noll, K. W. Henderson, *Chem. Commun.* **2007**, 5191–5193.
[11] For some examples of metal-organic frameworks containing magnesium, see: a) J. A. Rood, W. C. Boggess, B. C. Noll, K. W. Henderson, *J. Am. Chem. Soc.* **2007**, *129*, 13675–13682; b) J. A. Rood, B. C. Noll, K. W. Henderson, *Inorg. Chem.* **2006**, *45*, 5521–5528; c) M. Dincă, J. R. Long, *J. Am. Chem. Soc.* **2005**, *127*, 9376–9377; d) I. Senkovska, S. Kaskel, *Eur. J. Inorg. Chem.* **2006**, 4564–4569; e) D. R. Xiao, E. B. Wang, H. Y. An, Y. G. Li, Z. M. Su, C. Y. Sun, *Chem. Eur. J.* **2006**, *12*, 6528–6541.
[12] J. A. Rood, B. C. Noll, K. W. Henderson, *Inorg. Chem.* **2007**, *46*, 7259–7261.
[13] For instance, 2,4,6-trichloroaniline is more acidic than alkyl-substituted anilines by 5–6 pK_a units: a) B. G. Tehan, E. J. Lloyd, M. G. Wong, W. R. Pitt, E. Gancia, D. T. Manallack, *Quant. Struct.-Act. Relat.* **2002**, *21*, 473–485; b) F. G. Bordwell, D. J. Algrim, *J. Am. Chem. Soc.* **1988**, *110*, 2964–2968.
[14] A. Mueller, M. Krieger, B. Neumueller, K. Dehnicke, J. Magull, *Z. Anorg. Allg. Chem.* **1997**, *623*, 1081–1087.
[15] For related tetrameric aggregates, see: a) D. J. Eisler, T. Chivers, *Chem. Eur. J.* **2006**, *12*, 233–243; b) M. Westerhausen, N. Makropoulos, H. Piotrowski, M. Warchhold, H. Nöth, *J. Organomet. Chem.* **2000**, *614–615*, 70–73; c) G. Del Piero, M. Cesari, S. Cucinella, A. Mazzei, *J. Organomet. Chem.* **1977**, *136*, 265–274.
[16] P. A. Deck, *Chem. Eng. News* **2005**, *83*, 8.
[17] M. Fukuyo, K. Hirotsu, T. Higuchi, *Acta Crystallogr., Sect. B* **1982**, *38*, 640–643.
[18] E. F. Mooney, *An Introduction to ^{19}F NMR Spectroscopy*, Heyden & Son, London, **1970**.
[19] a) Z. Janas, L. B. Jerzykiewicz, P. Sobota, J. Utko, *New J. Chem.* **1999**, *23*, 185–188; b) B. F. Abrahams, T. A. Hudson, R. Robson, *J. Am. Chem. Soc.* **2004**, *126*, 8624–8625; c) M. Westerhausen, S. Schneiderbauer, J. Knizek, H. Nöth, A. Pfitzner, *Eur. J. Inorg. Chem.* **1999**, 2215–2220; d) D. B. Dell'Amico, F. Calderazzo, L. Labella, F. Marchetti, M. Martini, I. Mazzonzini, *C R. Chim.* **2004**, *7*, 877–878; e) V. C. Arunasalam, I. Baxter, J. A. Darr, S. R. Drake, M. B. Hursthouse, K. M. Abdul Malik, D. M. P. Mingos, *Polyhedron* **1998**, *17*, 641–657; f) P. Bailey, S. Parsons, D. Messenger, T. Borret, private communication, **2005**, CCDC-276714.
[20] F. H. Allen, *Acta Crystallogr., Sect. B* **2002**, *58*, 380–388.
[21] a) P. E. O'Connor, D. J. Berg, T. Barclay, *Organometallics* **2002**, *21*, 3947–3954; b) W. Liu, K. Welch, C. O. Trindle, M. Sabat, W. H. Myers, W. D. Harman, *Organometallics* **2007**, *26*, 2589–2597; c) D. Huang, K. B. Renkema, K. G. Caulton, *Polyhedron* **2006**, *25*, 459–468; d) M. E. van der Boom, Y. Ben-David, D. Milstein, *J. Am. Chem. Soc.* **1999**, *121*, 6652–6656; e) D. Ferraris, C. Cox, R. Anand, T. Lectka, *J. Am. Chem. Soc.* **1997**, *119*, 4319–4320; f) M. Mae, H. Amii, K. Uneyama, *Tetrahedron Lett.* **2000**, *41*, 7893–7896; g) H. Mii, T. Kobayashi, Y. Hatamoto, K. Uneyama, *Chem. Commun.* **1999**, 1323–1324; h) P. Mirosevic-Sorgo, B. C. Saunders, *Tetrahedron* **1959**, *5*, 38–43.
[22] a) A. Distler, F. L. Lohse, S. C. Sevov, *J. Chem. Soc., Dalton Trans.* **1999**, 1805–1812; b) J. Breau, W. Seidl, J. Senker, *Z. Anorg. Allg. Chem.* **2004**, *630*, 80–90; c) B. Neumueller, F. Gohlmann, *Z. Anorg. Allg. Chem.* **1993**, *619*, 718; d) H. Hao, H. W. Roesky, Y. Ding, C. Cui, M. Schormann, H.-G. Schmidt, M. Noltmeyer, B. Zemva, *J. Fluorine Chem.* **2002**, *115*, 143–147; e) F.-Q. Liu, A. Kuhn, R. Herbst-Irmer, D. Stalke, H. W. Roesky, *Angew. Chem. Int. Ed. Engl.* **1994**, *33*, 555–556.
[23] M. Gärtner, H. Görls, M. Westerhausen, *Dalton Trans.* **2008**, 1574–1582.
[24] Extended structures composed of trimeric magnesium building blocks are known: J. A. Rood, B. C. Noll, K. W. Henderson, *Main Group Chem.* **2006**, *5*, 21–30.
[25] S. Chadwick, U. Englich, M. O. Senge, B. C. Noll, K. Ruhlandt-Senge, *Organometallics* **1998**, *17*, 3077–3086.
[26] a) W. Clegg, K. W. Henderson, R. E. Mulvey, P. A. O'Neil, *J. Organomet. Chem.* **1992**, *439*, 237–250; b) W. Clegg, F. J. Craig, K. W. Henderson, A. R. Kennedy, R. E. Mulvey, P. A. O'Neil, D. Reed, *Inorg. Chem.* **1997**, *36*, 6238–6346; c) K. W. Henderson, W. J. Kerr, *Chem. Eur. J.* **2001**, *7*, 3430–3437.
[27] *APEX 2 and COSMO*, Bruker-Nonius AXS, Madison, Wisconsin, USA, **2005**.
[28] G. M. Sheldrick, *SADABS*, Bruker-Nonius AXS, Madison, Wisconsin, USA, **2004**.
[29] G. M. Sheldrick, *Acta Crystallogr., Sect. A* **2008**, *64*, 112–122.

Received: May 28, 2008
Published Online: July 25, 2008

 © 2008 Wiley-VCH Verlag GmbH & Co. KGaA, Weinheim